Biophysical Chemistry 142 (2009) 40–45

Contents lists available at ScienceDirect

Biophysical Chemistry

journal homepage: http://www.elsevier.com/locate/biophyschem

Explicit calcium bursting stochastic resonance

Ying Wang [a,*], Qianshu Li [b], Ji Luo [c]

[a] School of Chemistry and Pharmaceutical Engineering, Sichuan University of Science and Engineering, Sichuan, 643000, China
[b] Center for Computational Quantum Chemistry, South China Normal University, Guangzhou, 510006, China
[c] Sichuan University of Science and Engineering, Sichuan, 643000, China

ARTICLE INFO

Article history:
Received 7 October 2008
Received in revised form 27 January 2009
Accepted 2 March 2009
Available online 12 March 2009

Keywords:
Chemical Langevin method
Explicit stochastic resonance
Internal noise

ABSTRACT

In the present work the influence of internal noise resulting from small cell volume on bursting calcium oscillations is studied. With the internal noise switched on, the center of the main peak in the PSD (power spectrum density) was modified by internal noise. With increasing of the cell volume, the calculated signal-to-noise ratio (SNR) undergoes a maximum, which is referred in the present work as explicit bursting stochastic resonance. In addition, another quantity, the correlation time is used to measure the coherence of bursting oscillations. We demonstrate that the correlation time of the oscillations also exhibits a maximum at a certain cell volume.

1. Introduction

Bursting activity, which consists of alternating active and silent phases of spiking and quiescence, is a multi-time-scale phenomenon. Since it was firstly reported for the electrical activity of the neuron R15 [1,2], bursting activity has been studied experimentally [3–5] and theoretically [6–10] in the last three decades. For example, bursting has been observed in thalamic neurons [4], AB neurons [5], dopaminergic neurons [6], cerebellar Purkinje cells [11], and pancreatic β-cells [3,12]. Recently, bursting oscillations for intracellular Ca^{2+} signaling has attracted considerable attention. A significant part of signal transduction and controlling the complex behavior of biological systems is performed by the oscillatory changing of free cytosolic calcium concentration in excitable as well as in non-excitable cells [13]. These oscillations regulate many cellular processes ranging from egg fertilization to cell death [14]. Bursting oscillations of free cytosolic calcium have been found experimentally in many types of cells [15–17]. It has been shown that calcium bursting is more effective in maintaining glucose homeostasis than spikes [18,19], which suggests bursting being more helpful for insulin secretion [20].

Internal signal stochastic resonance (ISSR), i.e. noise-induced internal signal amplification [21,22] has been the topic of many investigations in the past both for its inherent interest and for its broad range of applications. With the development of SR studies, another type of ISSR, explicit internal signal stochastic resonance (EISSR) has been reported, where noise is directly added to an oscillatory state which is the intrinsic simple periodic signal of the system [23–26]. While most of the prior work only accounts for experimental external noise, the research attention has been gradually shifted to internal noise stochastic resonance (INSR). Internal noise resulting from the finite system size could induce stochastic oscillations, which show the best performance at a certain system size. However, seemingly little attention has been paid on the intrinsic noise amplification of the complex internal bursting signal.

In the present work, the reduced Kummer model [27] is used to get insight into the influence of internal noise on calcium bursting behavior. An internal noise-induced coherent motion was observed: with the increment of intrinsic noise level the evaluated signal-to-noise ratio (SNR) firstly increases and decreases slightly and then flattens out. The correlation time was also used to measure the coherence of bursting oscillations and the same results were obtained. Similar profiles of SNR and the correlation time demonstrated the occurrence of explicit bursting stochastic resonance.

2. Model description

The reduced Kummer model [27] describing the intracellular calcium oscillations in hepatocytes is used in this research. It is a core model and does not include all the processes that occur in calcium signal transduction but captures the fundamental dynamical characteristics of the complete model [28]. After the binding of an agonist to the extracellular side of a membrane-bound receptor molecule, the G_α subunit at the intracellular side of the receptor-coupled G-protein is activated. The activated G-protein in turn stimulates a phospholipase C (PLC), which leads to the production of IP_3, which diffuses through the cell and binds to receptors at the endoplasmic reticulum. This leads to the liberation of calcium from endoplasmic reticulum and in some cases to the inflow of calcium from extracellular space [28]. The concentration of IP_3 is not considered here as a separate

* Corresponding author. Tel.: +86 813 5594717.
E-mail address: ccbsmm@sina.com (Y. Wang).

0301-4622/$ – see front matter © 2009 Elsevier B.V. All rights reserved.
doi:10.1016/j.bpc.2009.03.002

variable. For simplicity, IP_3 is assumed to be in a quasistationary state. The reduced model of a single cell is presented as

$$\begin{aligned}\frac{dx}{dt} &= k_1 + k_2 x - \frac{k_3 xy}{x + K_4} - \frac{k_5 xz}{x + K_6},\\ \frac{dy}{dt} &= k_7 x - \frac{k_8 y}{y + K_9},\\ \frac{dz}{dt} &= k_{10} x - \frac{k_{11} z}{z + K_{12}},\end{aligned} \tag{1}$$

where x denotes the concentration of active G_α subunits of the G-protein, y refers to the concentration of active PLC, and z is the concentration of free calcium in the cytosol. More details of the model can be seen in Ref. [27]. Parameter values used here are: $k_1 = 0.212, k_3 = 1.52, K_4 = 0.19$, $k_5 = 4.88$, $K_6 = 1.18$, $k_7 = 1.24$, $k_8 = 32.24$, $K_9 = 29.09$, $k_{10} = 13.58$, $k_{11} = 153.0$, $K_{12} = 0.16$. Herein, k_2 is the concentration of agonist and is selected here as the control parameter.

For a typical living cell, such a deterministic description is not strictly valid due to the existence of considerable internal noise. Generally, one can describe the reaction system as a birth–death stochastic process governed by a chemical master equation [29], which describes the time evolution of the probability of a given number of molecules of reaction species. Although there is no procedure to solve this master equation analytically, it provides the starting point for numerical simulations. The exact stochastic simulation (ESS), introduced by Gillespie [30], implements such a master equation approach to stochastic chemical dynamics, which has been used as the stochastic method to describe the core model [27]. The ESS stochastically determines the reaction that takes place according to the probability of each reaction as well as the time interval to the next reaction. The numbers of molecules of different reacting species as well as the probabilities are updated at each time step. According to the ESS method, the number of active G_α units is introduced as X, the number of active PLC as Y, and the number of calcium ions in the cytosol as Z, such that the concentration of the reactants are $x = \frac{X}{LV}$, $y = \frac{Y}{LV}$ and $z = \frac{Z}{LV}$, where L is the Avogadro's number, V is the total cell volume, which is sometimes referred to as the system size and used to control the number of molecules present in the system, as described in Ref. [31]. The ESS method exactly accounts for the stochastic nature of the reaction events and has been widely used to study the properties and effects of internal noise in a variety of systems, but it is very time consuming and hardly applicable if the system size is large. In addition, it cannot afford us a clear perspective on the origin and magnitude of the internal noise in the system. Provided two dynamical conditions are satisfied, the microphysical premise from which the chemical master equation is derived leads directly to an approximate time-evolution equation of Langevin type. Condition (i): requires the time step dt to be small enough that the change in the state during $[t, t+dt]$ will be so slight that none of the propensity functions changes its value appreciably. Condition (ii): requires dt to be large enough that the expected number of occurrences of each reaction channel in $[t, t+dt]$ be much larger than one. The chemical Langevin (CL) method [32] has proven to be an efficient simulation algorithm [33–35] to account for internal noise. From the form of CLE, one can clearly find how the internal noise involved in the chemical reactions is related to the parameter values, the system size and the state variables that evolve with time. Here, the CL equations for the Kummer model can be described as

$$\begin{aligned}\frac{dX}{dt} &= (a_1 + a_2 - a_3 - a_4) + (\sqrt{a_1}\xi_1 + \sqrt{a_2}\xi_2 - \sqrt{a_3}\xi_3 - \sqrt{a_4}\xi_4),\\ \frac{dY}{dt} &= (a_5 - a_6) + (\sqrt{a_5}\xi_5 - \sqrt{a_6}\xi_6),\\ \frac{dZ}{dt} &= (a_7 - a_8) + (\sqrt{a_7}\xi_7 - \sqrt{a_8}\xi_8)\end{aligned} \tag{2}$$

where

$$a_1 = k_1 \cdot V,\ a_2 = k_2 x \cdot V,\ a_3 = \frac{k_3 xy}{x + K_4} \cdot V,\ a_4 = \frac{k_5 xz}{x + K_6} \cdot V,\ a_5 = k_7 x \cdot V,$$
$$a_6 = \frac{k_8 y}{y + K_9} \cdot V,\ a_7 = k_{10} x \cdot V,\ a_8 = \frac{k_{11} z}{z + K_{12}} \cdot V$$

$a_1 \cdots a_8$ are the transition rates of each reaction channel, as described in Table 1, where several reaction progresses have been eliminated according to the core model. $\xi_{i=1,\ldots,8}(t)$ are Gaussian white noises with $\langle \xi_i(t) \rangle = 0$ and $\langle \xi_i(t)\xi_j(t') \rangle = \delta_{ij}\delta(t-t')$. The additional terms compared to Eq. (1) describe internal noise, which is related to the cell volume V. Thereby V governs the amplitude of internal noise.

According to the relationship between the concentration and the molecule number, the corresponding macroscopic differential equations for the CL equations read

$$\begin{aligned}\frac{dx}{dt} &= \frac{1}{V}[(a_1 + a_2 - a_3 - a_4) + (\sqrt{a_1}\xi_1 + \sqrt{a_2}\xi_2 - \sqrt{a_3}\xi_3 - \sqrt{a_4}\xi_4)],\\ \frac{dy}{dt} &= \frac{1}{V}[(a_5 - a_6) + (\sqrt{a_5}\xi_5 - \sqrt{a_6}\xi_6)],\\ \frac{dz}{dt} &= \frac{1}{V}[(a_7 - a_8) + (\sqrt{a_7}\xi_7 - \sqrt{a_8}\xi_8)]\end{aligned} \tag{3}$$

From the form of Eq. (3) it can be found that the level of internal noise in the studied system is proportional to $1/\sqrt{V}$. If $V \to \infty$, Eq. (3) equal to the deterministic Eq. (1).

Table 1
Stochastic transition processes and corresponding rates.

Transition processes	Description	Transition rates
(1) $X \to X+1$	The spontaneous activation of G_α units	$a_1 = V \cdot k_1$
(2) $X \to X+1$	The accelerated formation of active G_α after binding of agonist to the membrane receptor	$a_2 = V \cdot k_2 x$
(3) $X \to X-1$	The inactivation of G_α units accelerated by active PLC	$a_3 = V \cdot \frac{k_3 xy}{x + K_4}$
(4) $X \to X-1$	Negative feedback of calcium-dependent kinase on G_α units	$a_4 = V \cdot \frac{k_5 xy}{x + K_6}$
(5) $Y \to Y+1$	The activation of PLC depends on the concentration of active G_α units	$a_5 = V \cdot k_7 x$
(6) $Y \to Y-1$	The enzymatic inactivation of PLC	$a_6 = V \cdot \frac{k_8 y}{y + K_9}$
(7) $Z \to Z+1$	The influx of calcium from the extracellular Space	$a_7 = V \cdot k_{10} x$
(8) $Z \to Z-1$	ATP-dependent ion pumps pump Ca^{2+} of cytosol back into the ER	$a_8 = V \cdot \frac{k_{11} z}{z + K_{12}}$

3. Results and discussion

With the variation of the control parameter k_2, the model is able to display spike and burst behaviors as appear in real cells [27]. We are primarily interested in the periodic bursting dynamics, and the control parameter k_2 is thus adjusted to 2.85. Most of the concepts about bursting oscillations come from neuron dynamics where bursting is an action potential one. In the present work, bursting is one mode of calcium oscillations, which is resulted from extracellular stimulation with such agonists as ATP and UTP in hepatocytes [27]. In order to elucidate the influence of internal noise, it is necessary to study the corresponding deterministic kinetics for comparison. Eq. (1) is integrated by using the explicit Euler method with a time step 0.0002 s, and the resulted time courses reported in Fig. 1a show the periodic bursting dynamics, where each main spike is followed by a series of secondary oscillations. The power spectrum density (PSD) in Fig. 1b shows the counterparts of the spikes in time courses. As can be readily observed there is one large peak and several low peaks at distinctively different frequencies. The bursting oscillations are consist of short trains of rapid spike oscillations intercalated by quiescent intervals, and they repeat periodically. Therefore Fig. 1b displays a

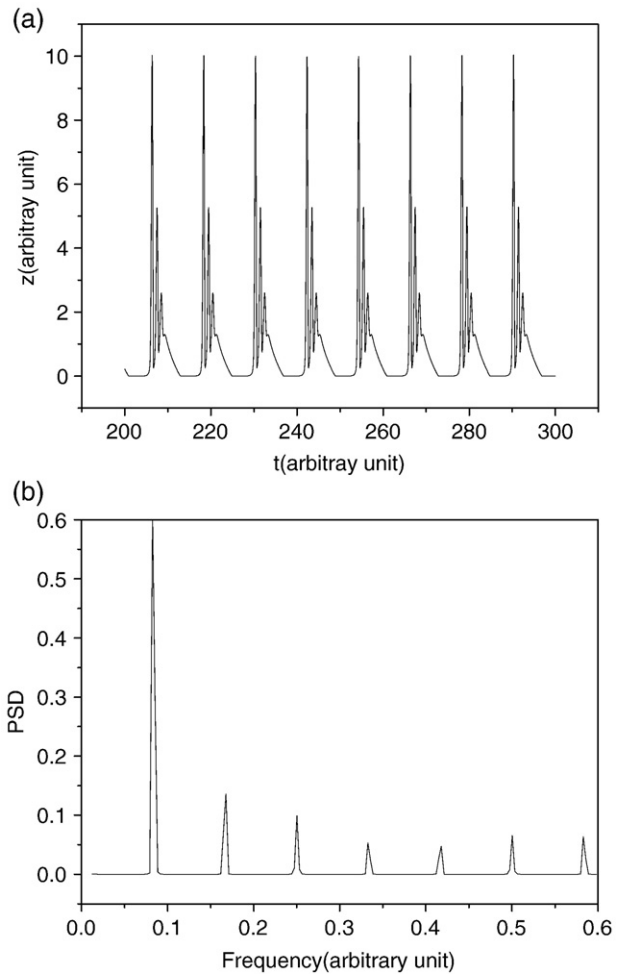

Fig. 1. Deterministic simulations of periodic bursting and the corresponding power spectrum density (PSD) of z at $k_2 = 2.85$.

power spectrum with strong peaks at the pacemaker frequency and its harmonics. The frequency of the main peak is viewed as the characteristic frequency here, and its exact value is 0.08239 s^{-1}.

Experimentally, Ca^{2+} dynamics is a stochastic system. Bursting may be completely due to noise in simple Ca^{2+} models, which do not exhibit bursting without noise. The diffusing species is cytosolic Ca^{2+} and the discrete stochastic sources are ion channels. Such systems generate spatiotemporal structures by wave nucleation due to thermal noise. In general, that leads to random spike sequences. The randomness does not arise from small numbers of molecules in the system, but rather from the fact that global events are initiated locally [36,37]. However, it is well known that the living cells involve a small number of interacting molecules due to their small volumes, hence, the state of the system is discrete and deterministic equations may give misleading results. The CL Eq. (3) is used here to take into account the intrinsic noise, and numerical simulations are performed by using the Eular–Maruyama method [38] with a time step of 0.0002 s. Temporal courses of z plotted in Fig. 2a–e show that with the addition of small magnitude intrinsic noise the bursting oscillations do not appear irregular. As the volume decreases, the level of internal noise increases. Thus, for the volume small enough, the level of internal noise becomes so high that bursting behavior is disrupted, resulting in random oscillations. As is described in Ref. [27], the model was constructed on the basis of previous experimental observations and data like those shown in Figs. 1 and 2 in Ref. [27], where the quantity is between 0 and 1000, and the unit of the calcium concentration is nM. Thus the peak values of free calcium concentrations in cytosol are around 1 mM. Therefore, the simulation results of the deterministic dynamics might be 1 mM, which are close to the experimental data. It is shown that the peak values in Fig. 2a–e of free cytosolic calcium concentration under the influence of internal noise approximate to the deterministic dynamics in Fig. 1a, and the peak values might be around 1 mM. The most interesting phenomenon is that with the decrease of cell volume the bursting oscillations disappear entirely and only spikes remain. It was assumed in Ref. [39] that in pancreatic β-cells, the Ca^{2+} influx into the ER via SERCA pumps depends linearly on the cytosolic Ca^{2+} concentration in the calcium-based PBM model

$$J_{\mathrm{SERCA}} = k_{\mathrm{SERCA}} c$$

where c is the cytosolic Ca^{2+} concentration, the parameter k_{SERCA} is expressed as a function of glucose concentration and is given by

$$k_{\mathrm{SERCA}} = \frac{k_1 c^2}{k_2^2 + c^2}(glu - glu_k)$$

where glu is the concentration of glucose, and glu_k is considered as the basal glucose level. Varying the glucose concentration means

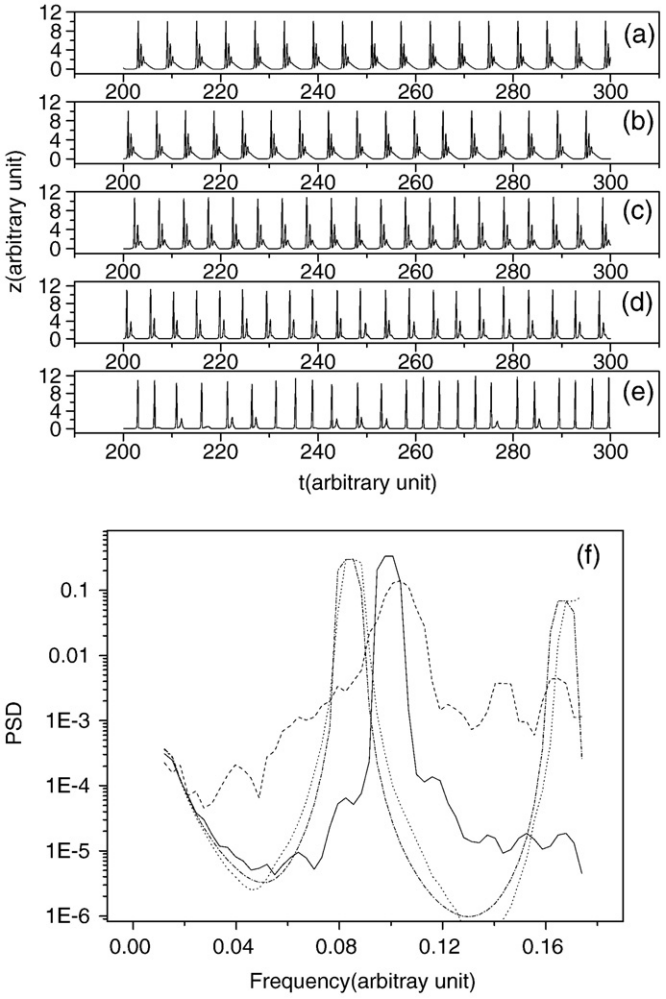

Fig. 2. Time series and the corresponding PSD of z at various volumes as $k_2 = 2.85$. (a) time series for z at $V = 10^{10}$, (b) time series for z at $V = 10^{6}$, (c) time series for z at $V = 10^{3.5}$, (d) time series for z at $V = 10^{2.8}$, (e) time series for z at $V = 10^{2.5}$ (f) the corresponding PSD for $V = 10^{10}$ (dash dotted line), $V = 10^{6}$ (dotted line), $V = 10^{3.5}$ (solid line) and $V = 10^{2.7}$ (dash line).

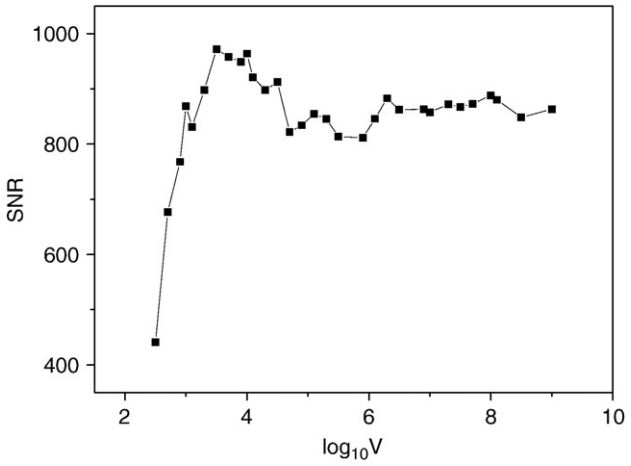

Fig. 3. The dependence of SNR on the cell volume V for z at $k_2 = 2.85$.

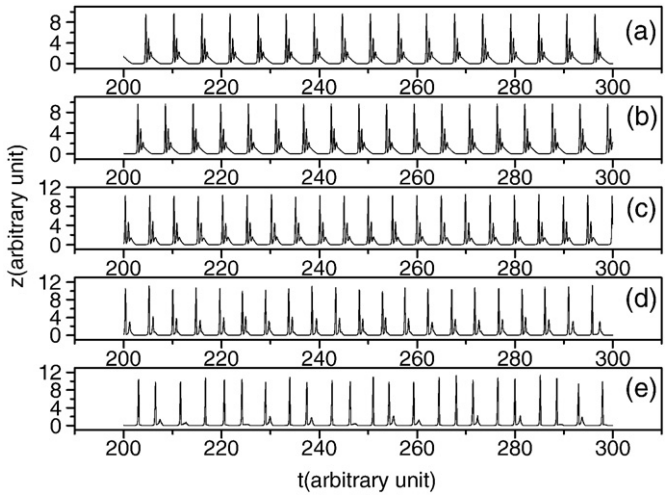

Fig. 5. Time series of z at various volumes as $k_2 = 2.80$. (a) time series for z at $V = 10^{10}$, (b) time series for z at $V = 10^{6}$, (c) time series for z at $V = 10^{3.5}$, (d) time series for z at $V = 10^{2.8}$, (e) time series for z at $V = 10^{2.5}$.

decreasing the cytosolic Ca^{2+} concentration. When IP_3 concentration is fixed, the bursting oscillations could be transferred into spiking by varying the glucose concentration. Herein, as V is smaller than $10^{2.8}$ internal noise transforms bursts to spikes ultimately, providing an alternative way to control the bursting and spiking activity. Furthermore, the smaller the volume is, the larger the frequency in the presence of noise becomes. It is probably due to that an increase of internal noise is equivalent to shifting k_2 to the fast oscillation region, hence one has larger frequency. Furthermore, a little change appears in the bursting amplitude. As $V \to \infty$ Eq. (3) equal to the deterministic Eq. (1). The frequency and the amplitude in the presence of internal noise approach that from the deterministic model. PSD of the main peak for increasing volumes are shown in Fig. 2f. Calcium oscillates with a much smaller period at $V = 10^{3.5}$ than at the other two volumes $V = 10^{6}$ and $V = 10^{10}$, confirmed by the larger frequency of the main peak at $V = 10^{3.5}$ in Fig. 2f. The characteristic frequencies in the presence of internal noise are all larger than the deterministic one, implying that the frequency of the main spectrum peak is considerably shifted. This indicates that internal noise shortens the period of bursting oscillation.

In addition, the main peak at $V = 10^{3.5}$ is a bit higher than that at the other three volumes. This phenomenon is reminiscent of EISSR, in which the response of a nonlinear system to a simple periodic signal is optimized by noise [23–26]. However, instead of optimizing an inherent simple periodic oscillation, here we have internal noise enhancement of the coherence of the periodic bursting. To demonstrate the occurrence of the resonance phenomenon, SNR is defined as that in Ref. [34], and the dependence of SNR on the cell volume is depicted in Fig. 3. The SNR is seen to exhibit the familiar stochastic resonance maximum as a function of the cell volume. Past the maximum, the SNR decrease to a constant. The emergent resonance could be viewed as explicit bursting stochastic resonance. Increasing internal noise here results in a less irregular output, and this paradoxical behavior might be due to the existence of two distinct time scales [40].

To further characterize the resonance quantitatively, we introduce another quantity, the characteristic correlation time, which is calculated as follows:

$$\tau_c = \int_0^{+\infty} d\tau \left(\frac{\langle \tilde{z}(t)\tilde{z}(t+\tau)\rangle}{(\langle \tilde{z}\rangle)^{\frac{1}{2}}} \right)^2 \tag{4}$$

with

$$\tilde{z} = z - \langle z \rangle \tag{5}$$

where $\langle \cdot \rangle$ denotes the average on time. In Fig. 4 we display the dependence of this quantity on the cell volume. As can be seen in Fig. 4, increasing V, thus decreasing internal noise, leads to a rapid rise of correlation time τ_c, indicating a higher coherence of the bursting behavior. Remarkably, however, a further increment of V does not always cause additional regularity, τ_c drops and finally reaches a constant. As the cell volume increases to an intermediate value, τ_c has a pronounced maximum, which illustrates that at a certain cell volume the regularity of the process is maximal. Comparing Fig. 3 with Fig. 4, it is obvious that in spite of some fluctuations in the SNR profile, the tendency is similar between the two quantities. Although bursting is transformed by internal noise as V is smaller than $10^{2.8}$, the bell shapes of Figs. 3 and 4 are not destroyed as V is larger than $10^{2.8}$, thus the explicit bursting stochastic resonance is further confirmed. When the control parameter is taken more deeply in the oscillatory regime, the results are usually different [41]. In the present work, $k_2 = 2.80$ is chosen to study the influence of internal noise in deep bursting region. The resulted time serials are shown in Fig. 5, and the corresponding

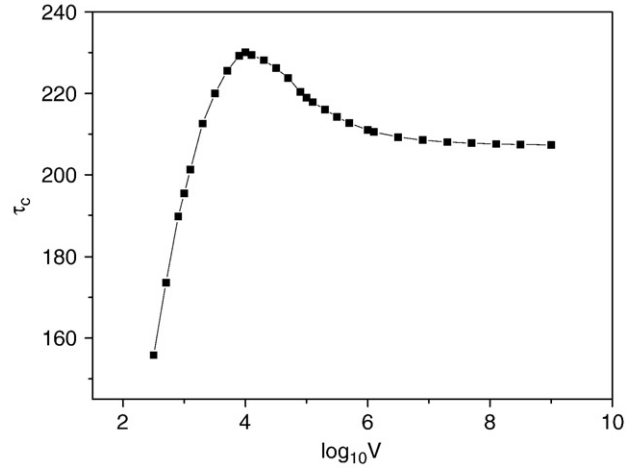

Fig. 4. The dependence of correlation time τ_c on the cell volume V for z at $k_0 = 2.85$.

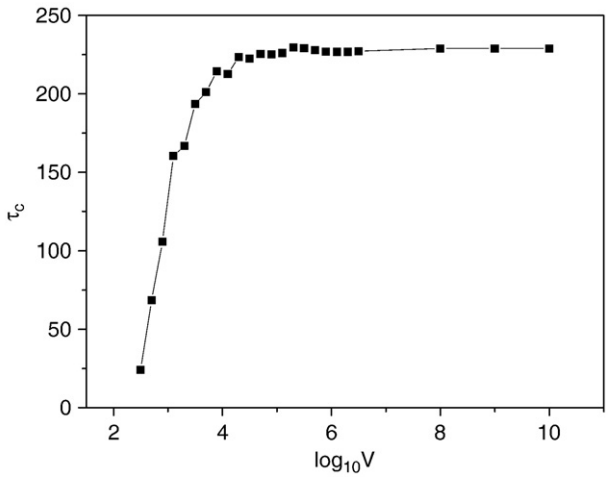

Fig. 6. The dependence of correlation time τ_c on the cell volume V for z at $k_2 = 2.80$.

correlation time is shown in Fig. 6. It is clear that internal noise does not enhance but destroy the regularity of the dynamic behavior. For larger internal noise, bursts change into spikes.

Stochastic resonance of bursting oscillations has been observed in pancreatic β-cells [42], where the internal noise resulting from the number of channels caused the emergence of bursting in the original spiking dynamics, and the bursting is the most desirable at a moderate channel number. In the present work, the internal noise originates from finite cell volume, and is taken into account in the original bursting oscillations. With the variation of the cell volume, the bursting behavior shows the best performance at a certain cell volume. Furthermore, this could be related to the recent publications [43,44]. In Ref. [43], Hou has studied the collective dynamics of an array of N-coupled cells, each of size V. Two size resonances are found, i.e., the regularity of calcium spikes induced by internal noise reach a maximum at an optimal cell size V when the network size N is fixed, and it also shows a maximum for an optimal N if V is fixed. In Ref. [44], Chen has reported that eternal noise has selective effects on system size bi-resonance induced by internal noise in the calcium system. Meanwhile, cell system may also automatically select an optimal cell size to obtain the best performance in the presence of external noise. In the two referenced papers, the internal noise has been considered in the steady state region in calcium system. However, internal noise is considered in the complex oscillation region in the present work, and bursting stochastic resonance is induced.

Signal transduction constitutes an important feature of biological systems: it provides the bridge between external stimuli and cellular reactions. The basis of the model in the present work is the scheme of signal transduction via calcium ion. Calcium signals encode and transmit information in frequency- or amplitude-modulation mode [45]. Frequency encoding is a strong dependence of the frequency of Ca^{2+} oscillations on the dose of the applied receptor agonist, whereas the oscillation amplitude remains nearly constant [46]. The oscillation frequency increases with strong stimulation. Internal noise should be considered in the cell. In the present work, internal noise increases bursting frequency, thus enlarge the influence of external stimulus. On the other hand, subtle modulation of the amplitude or the temporal/spatial presentation of Ca^{2+} signals can differentially regulate Ca^{2+}-sensitive processes within the same cell [47]. Understanding explicit bursting stochastic resonance in calcium system is expected to be applicable in cellular signaling like complex frequency–amplitude signal encoding and intracellular signal transduction.

4. Conclusion

In summary, the response of calcium bursting oscillations to internal noise is studied by solving mesoscopic chemical Langevin equations. Simulations show that internal noise shortens the period of bursting oscillations and the calculated SNR reaches a maximal at a certain internal noise (e.g. an optimal system volume) in a manner that resembles a stochastic resonance, which is typical for the explicit bursting stochastic resonance. The above results show that in the calcium system bursting oscillations could be optimized by internal noise. Then, another quantity, the correlation time was used to characterize the coherence of the bursting behavior, which is maximized for a system volume close to the one that maximizes the SNR. It may be an indication that an appropriate cell volume could lead to more regular dynamics. The study of explicit bursting stochastic resonance in calcium system might improve our understanding of several important biological phenomena in cellular signaling like complex frequency–amplitude signal encoding and intracellular signal transduction.

Acknowledgements

The present work was supported by the National Natural Science Foundation of China (Grant No. 20433050), the 111 Project in China (B07012), and the Talent Introduction Project of Sichuan University of Science and Engineering (072R11).

References

[1] F. Strumwasser, Types of information stored in single neurons, Invertebrate Nervous Systems: Their Significance for Mammalian Neurophysiology, The University of Chicago Press, Chicago, 1967.
[2] B. Alving, Spontaneous activity in isolated somata of *Aplysia* pacemaker neurons, J. Gen. Physiol. 51 (1968) 29–45.
[3] P.M. Dean, E.K. Matthews, Glucose-induced electrical activity in pancreatic islet cells, J. Physiol. 210 (1970) 255–264.
[4] V. Crunelli, J.S. Kelly, N. Leresche, M. Pirchio, The ventral and dorsal lateral geniculate nucleus of the rat: intracellular recordings in vitro, J. Physiol. 384 (1987) 587–601.
[5] R.M. Harris-Warrick, R.E. Flamm, Multiple mechanisms of bursting in a conditional bursting neuron, J. Neurosci. 7 (1987) 2113–2128.
[6] S.W. Johnson, V. Seutin, R.A. North, Burst firing in dopamine neurons induced by N-Methyl-D-Aspartate: role of electrogenic sodium pump, Science 258 (1992) 665–667.
[7] P. Smolen, D. Terman, J. Rinzel, Properties of a bursting model with two slow inhibitory variables, SIAM J. Appl. Math. 53 (1993) 861–892.
[8] M. Pernarowski, Fast subsystem bifurcations in a slowly varied Liénard system exhibiting bursting, SIAM J. Appl. Math. 54 (1994) 814–832.
[9] E.M. Izhikevich, Neural excitability, spiking and bursting, Int. J. Bifurc. Chaos 10 (2000) 1171–1266.
[10] E.M. Izhikevich, Subcritical elliptic bursting of Bautin type, SIAM J. Appl. Math. 60 (2000) 503–535.
[11] M.D. Womack, K. Khodakhah, Dendritic control of spontaneous bursting in cerebellar Purkinje cells, J. Neurosci. 24 (2004) 3511–3521.
[12] R. Bertram, L. Satin, M. Zhang, P. Smolen, A. Sherman, Calcium and glycolysis mediate multiple bursting modes in pancreatic islets, Biophys. J. 87 (2004) 3074–3087.
[13] M. Perc, M. Marhl, Different types of bursting calcium oscillations in non-excitable cells, Chaos, Solitons Fractals 18 (2003) 759–773.
[14] M.J. Berridge, M.D. Bootman, P. Lipp, Calcium – a life and death signal, Nature 395 (1998) 645–648.
[15] R. Jacob, Calcium oscillations in endothelial cells, Cell Calcium 12 (1991) 127–134.
[16] L. Sjödin, H.G. Dahlén, E. Gylfe, Calcium oscillations in guinea-pig pancreatic acinar cells exposed to carbachol cholecystokinin and substance P, J. Phys. 444 (1991) 763–776.
[17] A.K. Green, C.J. Dixon, A.G. Maclennan, P.H. Cobbold, M.J. Fisher, Adenine dinucleotide-mediated cytosolic free Ca^{2+} oscillations in single hepatocytes, FEBS Lett. 322 (1993) 197–200.
[18] P.A. Halban, C.B. Wollheim, B. Blondel, P. Meda, E.N. Niesor, D.H. Mintz, The possible importance of contact between pancreatic islet cells for the control of insulin release, Endocrinology 111 (1982) 86–94.
[19] D. Pipeleers, P.I. Veld, E. Maes, M.V.D. Winkel, Glucose induced insulin release depends on functional cooperation between islet cells, Proc. Natl. Acad. Sci. U.S.A. 79 (1982) 7322–7325.
[20] J.C. Henquin, H.P. Meissner, Significance of ionic fluxes and changes in membrane potential for stimulus-secretion coupling in pancreatic β-cells, Experientia, Experientia, vol. 40, 1984, pp. 1043–1052.
[21] G. Hu, T. Ditzinger, C.Z. Ning, H. Haken, Stochastic resonance without external periodic force, Phys. Rev. Lett. 71 (1993) 807–810.
[22] W.J. Rappel, S.H. Strogatz, Stochastic resonance in an autonomous system with a nonuniform limit cycle, Phy. Rev. E 50 (1994) 3249–3250.
[23] R. Zhu, Q.S. Li, Z.C. Liu, Explicit internal signal stochastic resonance in a chemical model driven by colored noise, Chem. Phys. Lett. 351 (2002) 410–416.

[24] Q.S. Li, R. Zhu, Stochastic resonance with explicit internal signal, J. Chem. Phys. 115 (2001) 6950-6595.
[25] Y.P. Li, Q.S. Li, Implicit and explicit internal signal stochastic resonance in calcium ion oscillations, Chem. Phys. Lett. 417 (2002) 498–502.
[26] Q.S. Li, H.Y. He, Signal transduction in a coupled hormone system: selective explicit internal signal stochastic resonance and its control, J. Chem. Phys. 123 (2005) 214905.
[27] U. Kummer, B. Krajnc, J. Pahle, A.K. Green, C.J. Dixon, M. Marhl, Transition from stochastic to deterministic behavior in calcium oscillations, Biophys. J. 89 (2005) 1603–1611.
[28] U. Kummer, L.F. Olsen, C.J. Dixon, A.K. Green, E. Bornberg-Bauer, G. Baier, Switching from simple to complex oscillations in calcium signaling, Biophys. J. 79 (2000) 1188–1195.
[29] N.G. Van Kampen, Stochastic Processes in Physics and Chemistry, North-Holland, Amsterdam, 1981.
[30] D.T. Gillespie, Exact stochastic simulation of coupled chemical reactions, J. Phys. Chem. 81 (1977) 2340–2361.
[31] M. Perc, M. Gosak, M. Marhl, Periodic calcium waves in coupled cells induced by internal noise, Chem. Phys. Lett. 437 (2007) 143–147.
[32] D.T. Gillespie, The chemical Langevin equation, J. Chem. Phys. 113 (2000) 297–306.
[33] H.Y. Li, Z.H. Hou, H.W. Xin, Internal noise stochastic resonance for intracellular calcium oscillations in a cell system, Phys. Rev. E 71 (2005) 061916.
[34] Z.H. Hou, H.W. Xin, Internal noise stochastic resonance in a circadian clock system, J. Chem. Phys. 119 (2003) 11508–11512.
[35] M. Yi, Y. Jia, Q. Liu, J.R. Li, C.L. Zhu, Enhancement of internal-noise coherence resonance by modulation of external noise in a circadian oscillator, Phys. Rev. E 73 (2006) 041923.
[36] M. Falcke, On the role of stochastic channel behavior in intracellular Ca^{2+} dynamics, Biophys. J. 84 (2003) 42–56.
[37] A. Skupin, H. Kettenmann, How does intracellular Ca^{2+} oscillate: by chance or by the clock? Biophys. J. 94 (2008) 2404–2411.
[38] D.J. Higham, An algorithm introduction to numerical simulation of stochastic differential equations, SIAM Rev. 43 (2001) 525–546.
[39] X. Zhan, D. Wu, L. Yang, Q. Liu, Y. Jia, Effects of both glucose and IP3 concentrations on action potentials in pancreatic beta-cells, Eur. Biophys. J. 36 (2007) 187–197.
[40] J.R. Pradines, G.V. Osipov, J.J. Collins, Coherence resonance in a noise-driven excitable and oscillatory system, Phys. Rev. E 60 (1999) 6407–6410.
[41] M. Gosak, M. Marhl, M. Perc, Chaos out of internal noise in the collective dynamics of diffusively coupled cells, Eur. Phys. J. B 62 (2008) 171–177.
[42] G.D. Vries, A. Sherman, Channel sharing in pancreatic β-cells revisited: enhancement of emergent bursting by noise, J. Theor. Biol. 207 (2000) 513–530.
[43] Z.H. Hou, J.Q. Zhang, H.W. Xin, Two system-size-resonance behaviors for calcium signaling: for optimal cell size and for optimal network size, Phys. Rev. E 74 (2006) 031901.
[44] H.S. Chen, J.Q. Zhang, J.Q. Liu, Selective effects of external noise on Ca^{2+} signal in mesoscopic scale biochemical cell systems, Biophys. Chem. 125 (2007) 397–402.
[45] S. Krauss, M.D. Brand, Quantitation of signal transduction, FASEB J. 14 (2000) 2581–2588.
[46] A. Politi, L.D. Gaspers, A.P. Thomas, T. Hofer, Models of IP_3 and Ca^{2+} oscillations: frequency encoding and identification of underlying feedbacks, Biophys. J. 90 (2006) 3120–3133.
[47] M.D. Bootman, T.J. Collins, et al., Calcium signaling – an overview, Semin. Cell Dev. Biol. 12 (2001) 3–10.